Electric Power Systems Research 103 (2013) 168–177

Contents lists available at SciVerse ScienceDirect

Electric Power Systems Research

journal homepage: www.elsevier.com/locate/epsr

Extended Kalman filtering based real-time dynamic state and parameter estimation using PMU data

Lingling Fan*, Yasser Wehbe

Department of Electrical Engineering, University of South Florida, Tampa, FL 33620, USA

ARTICLE INFO

Article history:
Received 23 January 2013
Received in revised form 26 May 2013
Accepted 27 May 2013
Available online 30 June 2013

Keywords:
Power system modeling
Extended Kalman filter
Phasor measurement units
Dynamic state estimation
Dynamic parameter estimation

ABSTRACT

This paper proposes extended Kalman filtering (EKF) based real-time dynamic state and parameter estimation using phasor measurement unit (PMU) data. In order to reduce computing load, model decoupling technique is used where measurements (real power, reactive power, voltage magnitude and phase angle) from a PMU are treated as inputs and outputs from the system. Inputs are real and reactive powers while outputs are voltage magnitude phase angle. EKF is implemented using a second-order swing equation and a classical generator model to estimate the two dynamic states (rotor angle and rotor speed) and unknown parameters, e.g., mechanical power, inertia constant, damping factor and transient reactance. An EKF algorithm is developed using model decoupling technique for real-time estimation of states and parameters related to electromechanical dynamics. The EKF based estimation can estimate two dynamic states along with four unknown parameters.

1. Introduction

Phasor measurement units (PMU) equipped with GPS antennas measure three-phase instantaneous voltages and currents and calibrates phasors. These phasors are transmitted with time stamps and called synchrophasors. Synchrophasors have many applications that enhance situation awareness of the power grid. The Department of Energy has supported PMU installation around the US through the Smart Grid Investment Grant (SGIG) with a plan for thousands of PMUs to be installed in the US over the next several years. Effective use of the PMU data to enhance power system situation awareness and security is of key interest to power system operators.

State estimation can be generally classified into two categories: steady state and dynamic. Conventional state estimation belongs to the first category, where bus voltages and phase angles are estimated every 5 min and the estimation handles *steady state* power flow problems. The measurements could be active power, reactive power and voltage magnitude. With phasor measurements, steady state estimation can incorporate direct phasor measurements and formulate least square estimation problems [1–3].

This paper deals with dynamic state and parameter estimation employing PMU data. The current data in Eastern Interconnection collected by the RTDMS database [4] has a 30 Hz sampling rate. This is a much faster sampling rate compared to that of conventional state estimation (0.2 Hz sampling rate). With such a sampling rate, estimation of dynamic states and parameters related to critical low frequency electromechanical dynamics becomes feasible. Two applications can be envisioned for PMU data based dynamic estimation. The *first* one is in generator model and parameter estimation. NERC MOD-013 [5] compliance requires unit-specific dynamics data shall be reported. These data include generator (inertia constant, damping coefficient, direct and quadrature axes reactances and time constants), excitation systems, voltage regulators, turbine-governor systems, power system stabilizers, and other associated generation equipment. Currently, the data required by NERC have to be obtained by bringing a unit offline and conducting tests. The research problem investigated in this paper can provide some of the data required by NERC MOD-013 and therefore have a practical application in online generator parameter estimation without interrupting units operation. The *second* application is subsystem identification. Instead of just one generator unit, a subsystem consisting of multi units can be estimated with PMU data.

Synchronous generator parameter estimation has been investigated in the literature. Based on the data used, the methods can be classified into: time-domain data based [6–18] and frequency response data based [19–22] methods. Based on the nature of the measurements, there are digital fault recorder data with high sampling rate based estimation for generator electrical parameters [15–18], and other online tests based methods such as short circuit tests [7,9], step or binary sequence inputs into excitation [8,11,12], and offline tests based [19–22] methods. Based on the scope of the estimation, some focus on electrical parameters (e.g., *qd*-axis

* Corresponding author. Tel.: +1 813 974 2031; fax: +1 813 974 5250.
E-mail address: linglingfan@usf.edu (L. Fan).

0378-7796/$ – see front matter © 2013 Elsevier B.V. All rights reserved.
http://dx.doi.org/10.1016/j.epsr.2013.05.016

resistances and inductances) only [7,9,13–22], while [8,10–12] estimate both electrical and mechanical parameters. Based on the estimation methods, then there are at least two major systematic methods to deal with differential equation model estimation: least square estimation [6–9,12,14,19,20] and Kalman filter estimation [10,11].

PMU data based estimation problems fall into the category of online, time-domain, and electro-mechanical dynamics related problems.

In the literature, a synchronous generators' parameters can be estimated accurately if given sufficient measurements. For example, in [8], a third-order machine model parameters (H, D, T'_{do}) are estimated based on the measurements of the terminal voltage, output power, angle given a step response in excitation system. In [11], electrical and mechanical parameters of a generator can be estimated given measurements from filed current, terminal current, terminal powers, rotor angle and rotor speed. In [12], electrical and mechanical parameters of a generator can be estimated given measurements of three-phase currents, line voltages, and field voltage. Ref. [6] indicates that machine circuit parameters and mechanical system parameters can be estimated given different sets of measurements.

Unlike the estimation problems in the literature, PMU data are limited to voltage, current phasors in addition to frequency, power and time. We cannot obtain measurements as much as we want such as in [11,12]. Secondly, unlike the tests conducted in [8,10,12], the trigger of transients is unknown. Field current and voltage measurements are not available.

Therefore, PMU data based estimation problems are limited to state estimation only [23,24] or state/parameter estimation for 2nd order mechanical system [25–29]. The above investigation all applies Kalman filtering technology in estimation. There are other methods in PMU data based estimation method designated for a special system, e.g., [30] investigates a radial system estimation problem. In this paper, a general approach that can be applied for any system is sought.

EKF approach is adopted in this paper to estimate a generator's model and parameters. Unlike least squared estimation which uses a time window of data, EKF estimation uses the current step measurements and prediction. Hence the data storage requirement is very low. This approach can also be used to estimate a reduced-order model, which can represent a subsystem. In addition, to reduce the computation burden, instead of estimating the entire system, only a subsystem or a generator is estimated. The generator is however interconnected to the grid. Therefore, a model-decoupling method will be introduced in this paper to decouple the subsystem model from the grid by treating a subset of measurements as inputs to the model.

Model decoupling technique has been employed in decentralized nonlinear control and subsystem model validation [26,28,31,32]. A subsystem's model will be independent from the rest of the system as long as the interfacing variables with the rest of the system can be measured and used as the input for a local decentralized controller. In [31], terminal voltage is the interfacing variable. In [32], currents are the interfacing variables. In model validation, a technique used in subsystem model validation is called "event play back" [26,28]. In "event play back," the objective is to estimate the parameters for a dynamic model which represents a synchronous generator or a subsystem. Measurements at the terminal bus will be separated into two groups. One group (voltage magnitude and phase angle) is treated as the input signals to the dynamic model and the other group (real and reactive power) is treated as the measurements in the EKF algorithm. Using such a technique, there is no longer the need to deal with the dynamic model of an entire power system; rather, second-order dynamic models will be used in the EKF in parallel.

This paper will propose a model decoupling method and implement EKF to estimate dynamic states and parameters related to electromechanical dynamics. Compared to the most recent work on EKF implementation in PMU data for dynamic state estimation in [23,26], the contribution of this paper is two-fold:

- The estimation can handle *more parameters*. The problem presented in this paper is more comprehensive where two states and four unknown parameters will be estimated. Estimated problem in [23] deals with four dynamic states (δ, ω, E'_q and E'_d) and one unknown parameter (excitation voltage E_{fd}). All other parameters such as inertia constant H, damping factor D and reactances are assumed to be known. Estimation of H and D have shown to be more difficult than other parameters [26] since nonlinearity is introduced and there will be more linearized error in EKF prediction. EKF-based estimation in [26] assumes the mechanical power for a generator is known and three parameters H, D and x'_d are estimated. This paper will tackle four-parameter and five-parameter estimation problems.
- The estimation can handle *modeling errors*. The model used in this paper is the simplest for a synchronous generator. However the estimation will be tested against simulation data from more sophisticated model to demonstrate the robustness of the proposed estimation. This is a step further than research in [23–29] where estimation model is the same as the simulation model with white noise added in measurements. In this paper, the estimation is tested against unmodeled dynamics which are no longer white noises.

The following sections will explain the basic EKF algorithm (Section 2), model decoupling and EKF implementation (Section 3). Case studies will be present in Section 4. Section 5 concludes the paper.

2. Basic algorithm of EKF

Kalman filter theory was developed by R. Rudolf Kalman in late 1950s and can be considered as a type of observers for linear dynamic systems perturbed by white noise by use of white noise polluted measurements [33]. Kalman filter is suitable for real time estimation since the estimation is done for any instantaneous time. EKF is a discrete Kalman filter adapting to nonlinear system estimation through linearization.

For a nonlinear dynamic system described by differential algebraic equations (DAEs) in (1) and further in discrete form in (2), the purpose of EKF is to minimize the covariance of the mismatch between the estimated states and the states.

$$\begin{cases} \dfrac{d\mathbf{x}}{dt} = f_c(\mathbf{x}, \mathbf{y}, \mathbf{u}, \mathbf{w}) \\ 0 = g_c(\mathbf{x}, \mathbf{y}, \mathbf{u}, \mathbf{v}) \end{cases} \tag{1}$$

where the $\mathbf{x}$ vector represents the state variables, the $\mathbf{y}$ vector represents the algebraic variables, $\mathbf{u}$ is the vector of input variables, $\mathbf{w}$ and $\mathbf{v}$ are processing noise and measurement noise. The subscript "c" denotes the continuous form. The discrete form of (1) is shown as follows:

$$\begin{cases} \mathbf{x}_k = \mathbf{x}_{k-1} + f_c(\mathbf{x}_{k-1}, \mathbf{u}_{k-1}, \mathbf{w}_{k-1})\Delta t \\ \equiv f(\mathbf{x}_{k-1}, \mathbf{u}_{k-1}, \mathbf{w}_{k-1}) \\ 0 = g_c(\mathbf{x}_k, \mathbf{y}_k, \mathbf{u}_k, \mathbf{v}_k) \Rightarrow \mathbf{y}_k = h(\mathbf{x}_k, \mathbf{u}_k, \mathbf{v}_k) \end{cases} \tag{2}$$

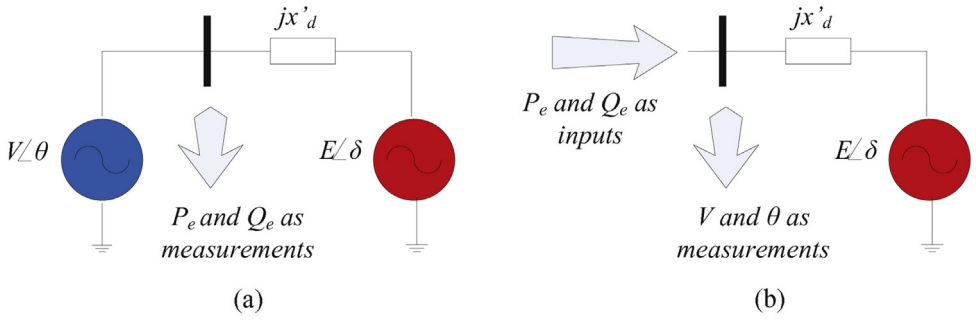

Fig. 1. (a) Model decoupling using V and θ as inputs while P_e and Q_e as measurements. (b) Model decoupling using P_e and Q_e as inputs while V and θ as measurements.

The EKF problem can accommodate parameter estimation by adding "auxiliary states" where $x_k = x_{k-1}$. The EKF problem can be solved in a two-step process [34]:

$$\text{Prediction}: \quad \begin{cases} \hat{\mathbf{x}}_k^- = f(\hat{\mathbf{x}}_{k-1}, h(\hat{\mathbf{x}}_{k-1}, \mathbf{u}_{k-1}), \mathbf{u}_{k-1}, 0) \\ P_k^- = A_k P_{k-1} A_k^T + W_k Q_{k-1} W_k^T \end{cases} \tag{3}$$

$$\text{Correction}: \quad \begin{cases} K_k = P_k^- H_{z,k}^T (H_{z,k} P_k^- H_{z,k}^T + V_k R_k V_k^T)^{-1} \\ \hat{\mathbf{x}}_k = \hat{\mathbf{x}}_k^- + K_k(\mathbf{z}_k - h(\hat{\mathbf{x}}_k^-, \mathbf{u}_k, 0)) \\ P_k = (I - K_k H_{z,k}) P_k^- \end{cases} \tag{4}$$

where the superscript $^-$ denotes a *priori* state, A_k and W_k are the process Jacobians at step k, P_k is a co-variance matrix of the state estimation error and is also called gain factor matrix, and Q_k is the process noise covariance at step k. $H_{z,k}$ and V_k are the measurement Jacobians at step k, and R_k is the measurement noise covariance at step k.

$$A = \frac{\partial f}{\partial \mathbf{x}}, \quad H_z = \frac{\partial h}{\partial \mathbf{x}}, \quad W = \frac{\partial f}{\partial \mathbf{w}}, \quad V = \frac{\partial h}{\partial \mathbf{v}}. \tag{5}$$

3. Model decoupling and EKF implementation

3.1. Model decoupling

The technique used in subsystem model validation called "event play back" [26,28] has the potential to decouple the EKF problem by better use of PMU data. One group is treated as the input signals to the dynamic model and the other group is treated as the measurements in the EKF problem. Using such a technique, there is no longer the need to deal with the dynamic model of an entire power system. Rather, *small-scale* dynamic models will be used in the EKF *in parallel*.

Each PMU provides voltage phasor and current phasor. From the provided data, active power P and reactive power Q can be computed. In this application, we consider PMU provides four data sets: voltage magnitude (V), voltage phase angle (θ), active power (P_e) and reactive power (Q_e). Only positive sequence data from PMUs are used in this application since it is reasonable to assume that transmission systems are operated under balanced conditions for majority of the time. The dynamic model of each generator (modeled as a constant voltage behind a transient reactance) is expressed as follows:

$$\begin{cases} \dfrac{d\delta}{dt} = \omega - \omega_0 \\ \dfrac{d\omega}{dt} = \dfrac{\omega_0}{2H}(P_m - P_e - D(\omega - \omega_0)) \\ \dfrac{d\omega}{dt} = \dfrac{\omega_0}{2H}\left(P_m - \dfrac{EV}{x'_d}\sin(\delta - \theta) - D(\omega - \omega_0)\right) \end{cases} \tag{6}$$

The vector of the state variables is $\mathbf{x} = [\delta, \omega]^T$ (δ-rotor angle and ω-rotor speed). E and P_m are internal voltage and mechanical power. The coupling between a generator and network can be viewed at two levels: at electric level and at electro-mechanical level. At electrical level, the generator is modeled as a voltage source behind impedance. A network voltage and current relationship can be setup $YV = I$. At the electro-mechanical level, the machine speed is influenced by the electric network through the electric power exported. The mechanical power is assumed to be constant or the slow dynamics of the mechanical system is ignored. Fast dynamics in the damping windings are ignored. Further, field flux is assumed to be constant.

There are two ways to decouple the model using PMU measurements as shown in Fig. 1. Method a treats the terminal voltage phasor (V and θ) as the input signal and the power P_e and Q_e as the measurements. Method B treats the power as input signals and the voltage phasor as the measurements. When P_e and Q_e are treated as the input for the model presented in (6), (6) can then be considered as a stand-alone dynamic model. On the other hand, if P_e and Q_e are not treated as the input, each generator will be dominated by its dynamic equation as (6). These equations are coupled by the expression of electric power.

The relationship of P_eQ_e, $V\theta$ and other state variables can be found in the following two equations.

$$\begin{cases} P_e = \dfrac{EV}{X'_d}\sin(\delta - \theta) \\ Q_e = \dfrac{-V^2 + EV\cos(\delta - \theta)}{X'd} \end{cases} \tag{7}$$

Method A has been applied by the PNNL group in [28,29]. Method B, however, has not been investigated. A significant difference of Methods A and B resides in the prediction step rotor speed computation.

$$\begin{aligned} &\omega_{k+1} = \frac{\omega_0}{2H_k}\left(P_{m,k} - \frac{EV_k \sin(\delta_k - \theta_k)}{x'_{d,k}} - D_k\left(\frac{\omega_k}{\omega_0} - 1\right)\right)\Delta t + \omega_k, \quad \text{Method } A \\ &\omega_{k+1} = \omega_k + \frac{\omega_0}{2H_k}\left(P_{m,k} - P_{e,k} + D_k\left(\frac{\omega_k}{\omega_0} - 1\right)\right)\Delta t, \quad \text{Method } B \end{aligned} \tag{8}$$

Method A relies on the voltage measurement, phase angle measurement, and transient reactance estimation to compute the

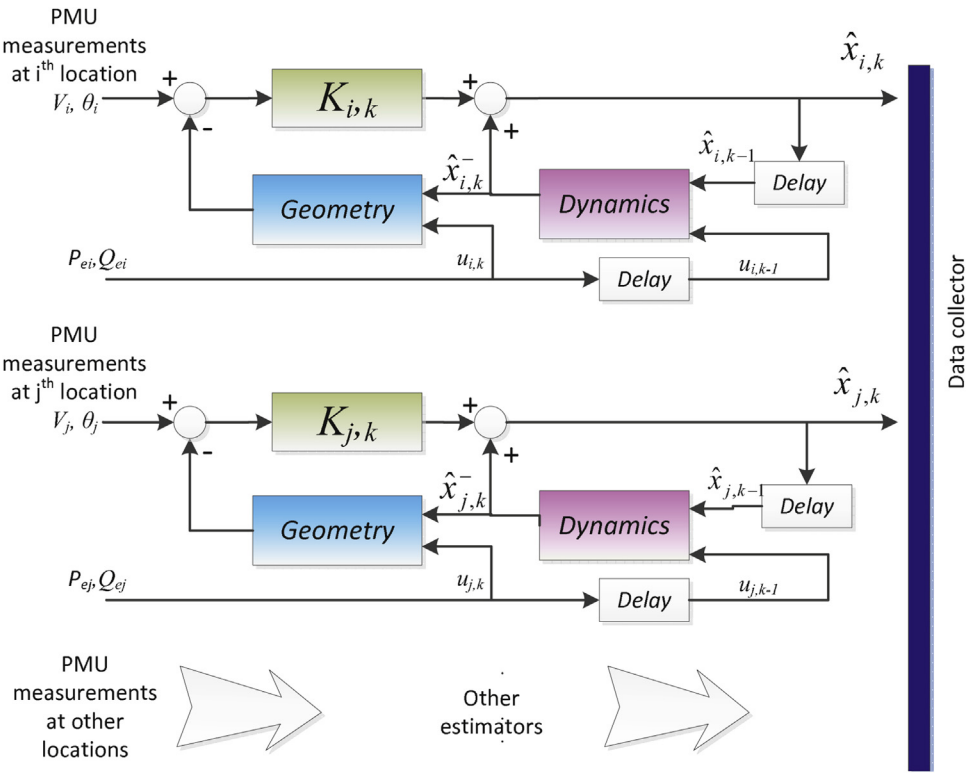

Fig. 2. Kalman filtering technology using PMU data.

electric power in the prediction step. The expression for power is only accurate for a classical generator model. In addition, when the transient reactance is unknown, there will be significant errors in computing power. Compared to Method *A*, Method *B* uses the power measurements as the input for the model. The accuracy of the rotor speed prediction is greatly improved. Method *A* has been applied in [26,28] and there are two limitations: (1) It cannot handle modeling error. In [26,28], the simulation model and the estimation model are the same classical model. (2) It cannot handle four unknown parameters. It can only handle three parameters.

Therefore, in this paper, Method *B* is used as the model decoupling technique for EKF implementation. The EKF implementation is shown in Fig. 2 where PMU data are separated into two groups (P_eQ_e as inputs and $V\theta$ as measurements). The dynamics block performs prediction using system equations while the geometry block computes the estimated measurements based on the *priori* states. A Kalman filter gain is used to correct the *priori* state with the error between the measurements and their estimation.

3.2. EKF implementation

In this subsection, detailed mathematical model of the EKF will be given. The states and parameters to be estimated are the rotor angle (δ), the rotor speed (ω), the mechanical power (P_m), the inertia constant H, the damping factor D and the transient reactance x'_d. PMU can give measurements for the terminal voltage magnitude, voltage phase angle, real power and reactive power. The real and reactive power are treated as the input. The voltage magnitude and voltage phase angle are treated as the outputs or measurements. The discrete model for the estimation system is describe as follow:

$$\begin{cases} \delta_{k+1} = \delta_k + (\omega_k - \omega_0)\Delta t + w_1 \\ \omega_{k+1} = \omega_k + \dfrac{\omega_0}{2H_k}(P_{m,k} - P_{e,k})\Delta t + D_k(\omega_k - \omega_0)\Delta t + w_2 \\ P_{m,k+1} = P_{m,k} + w_3 \\ H_{k+1} = H_k + w_4 \\ D_{k+1} = D_k + w_5 \\ x'_{d,k+1} = x'_{d,k} + w_6 \end{cases} \tag{9}$$

where $P_{e,k}$ is the input of the system, w_i are the noise to represent un-modeled dynamics and ω_0 is the nominal frequency.

The Jacobian matrix A is given by

$$A = \begin{bmatrix} 1 & \Delta t & 0 & 0 & 0 & 0 \\ 0 & 1 - \dfrac{D\omega_0\Delta t}{2H} & \dfrac{\omega_0\Delta t}{2H} & A_{24} & A_{25} & 0 \\ 0 & 0 & 1 & 0 & 0 & 0 \\ 0 & 0 & 0 & 1 & 0 & 0 \\ 0 & 0 & 0 & 0 & 1 & 0 \\ 0 & 0 & 0 & 0 & 0 & 1 \end{bmatrix} \tag{10}$$

where

$$A_{24} = -\frac{P_m - P_e - D(\omega - \omega_0)}{2H^2}\omega_0\Delta t$$

$$A_{25} = \frac{-(\omega - \omega_0)}{2H}\omega_0\Delta t$$

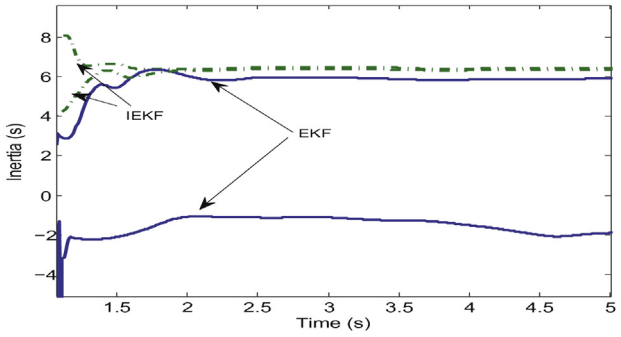

Fig. 3. Estimation results of the inertia constant based on Set 1 data using EKF and iterative EKF.

The measurement sensitivity matrix H_z can be found from the implicit functions (7).

$$H_z = \begin{bmatrix} \frac{\partial V}{\partial \delta} & \frac{\partial V}{\partial \omega} & \frac{\partial V}{\partial P_m} & \frac{\partial V}{\partial H} & \frac{\partial V}{\partial D} & \frac{\partial V}{\partial x'_d} \\ \frac{\partial \theta}{\partial \delta} & \frac{\partial \theta}{\partial \omega} & \frac{\partial \theta}{\partial P_m} & \frac{\partial \theta}{\partial H} & \frac{\partial \theta}{\partial D} & \frac{\partial \theta}{\partial x'_d} \end{bmatrix} = \begin{bmatrix} 0 & 0 & 0 & 0 & \frac{\partial V}{\partial x'_d} \\ 1 & 0 & 0 & 0 & \frac{\partial \theta}{\partial x'_d} \end{bmatrix} \quad (11)$$

where

$$\frac{\partial V}{\partial x'_d} = \frac{((-Q_e E^2 - 2x'_d P_e^2)/\sqrt{f_1}) - 4Q_e}{\sqrt{f_2}} \quad (12)$$

$$\frac{\partial \theta}{\partial x'_d} = \frac{2P_e f_2 - P_e x'_d(((-4Q_e E^2 - 8x'_d P_e^2)/\sqrt{f_1}) - 4Q_e)}{f_2\sqrt{E^2 f_2 - 4P_e^2 x'^2_d}} \quad (13)$$

where

$$f_1 = -4Q_e x'_d E^2 + E^4 - 4x'_d P_e^2 \quad (14)$$

$$f_2 = 2\sqrt{f_1} + 2E^2 - 4Q_e x'_d \quad (15)$$

3.3. Iterated extended Kalman filter (IEKF)

In order to achieve better convergence, iterative EKF [34] is adopted. For each time step, previously there is one prediction and one update step. In iterative EKF setup, for each time step, there will be iterations to update the Jacobian matrices and calculate estimated measurements. IEKF requires more computation time in correction step compared to EKF.

EKF algorithm expands the measurement function h_k in (2) in the *correction* stage around x_k^- obtained as the best estimation of x from the *prediction* phase:

$$h(x_k, u_k, v_k) = h(\hat{x}_k^-, u_k, 0) + H_z(\hat{x}_k - x_k^-) + v_k \quad (16)$$

However, after the correction phase we have a better estimate of x_k as in $\hat{x}_k$. Using such estimate $\hat{x}_k$ in (16) instead of $\hat{x}_k^-$ could decease the linearization errors in the rest of the estimation process and improve the estimate $\hat{x}_k$ of the correction phase. Iterative extended Kalman filter (IEKF) is based on repeating the linearization of h and the *correction* phase on the improved estimate $\hat{x}_k^i$ where i is the number of the iteration.

A comparison of the estimation results obtained by EKF and iterative EKF for the case study presented in Section 4 is shown in Fig. 3.

Two initial guesses of H are used for each estimation. It is found that iterative EKF can significantly increase the convergence rate toward the accurate parameter. The initial guess of H is set to be 4 pu.s or 8 pu.s. In both cases, ITEF can find the accurate estimation within 2 s. EKF however cannot reach the accurate estimation in 10 s. In addition, when the initial guess is 8 pu.s, EKF gives an estimation of a negative number.

In the following case studies, IEKF will be used.

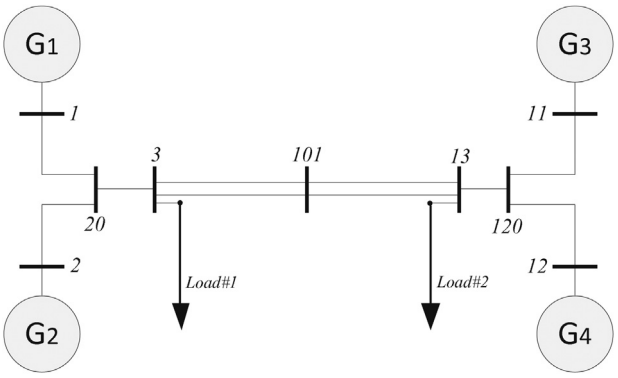

Fig. 4. The study system.

4. Case studies

The study system is the classic two-area four-machine system in the literature [35] (Fig. 4). A three-phase fault occurs at $t = 1$ s on Load 1 bus. Load 1 is tripped after 0.1 s. Voltage phasor data and current phasor data from a generator terminal bus will be recorded. The sampling interval is 0.01 s. The simulation is carried by Power System Toolbox [36]. The recorded data will be used to test the EKF methods. Four sets of simulation data will be recorded. To determine electromechanical states and parameters, the data contain obvious electromechanical oscillations are desired. On the other hand, measurements from digital fault recorders with high sampling rates and lasting less than 1 second are dominated by electromagnetic dynamics and hence are not suitable for the proposed method.

- Set 1: In the first set, classical generator models are used in simulations. Hence the Kalman filter dynamic model is exactly same as the simulation model. The machine parameters are $H = 6.5$ s, $D = 6$ pu, $x'_d = 0.25$ pu, $E = 1.08$ pu, and $P_m = 0.85$ pu.
- Set 2: In the second set, the damping is reduced to zero in the swing equation. The simulation model is same as the estimation model.
- Set 3: In the third set, subtransient generator model [37] including dynamics in damping windings and field winding is used. The damping factor is zero. The simulation model is more sophisticated than the estimation model.
- Set 4: In the fourth set, subtransient generator model is used. The damping factor is six. Automatic voltage regulator (AVR) is enabled to get a stable system response.

When damping factor is zero, the system lacks damping and the PMU data in Fig. 5 presents obviously poor damped oscillations. Testing on those data can demonstrate that the proposed algorithm can converge well even the system is poorly damped.

At least two initial guesses will be used to demonstrate if EKF can converge to a same estimation or not. For the two states and four parameter estimation problem, Sets 1–4 are used. For the two states and five parameter estimation problem, Sets 1 and 4 are tested.

The PMU data (V, θ, P_e, Q_e) for the four sets are plotted in Fig. 5. Among them, the power are used as input to the estimation model while the voltage phasor is treated as the measurements.

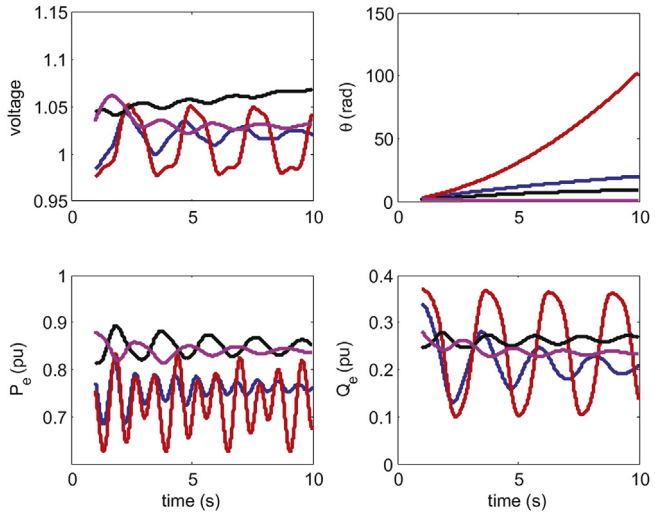

Fig. 5. The PMU data V, θ, P and Q. P and Q are treated as the input to the estimation model while V and θ are treated as the measurement of the output of the estimation model. Set 1: red. Set 2: blue. Set 3: black. Set 4: magenta. (For interpretation of the references to color in this figure legend, the reader is referred to the web version of the article.)

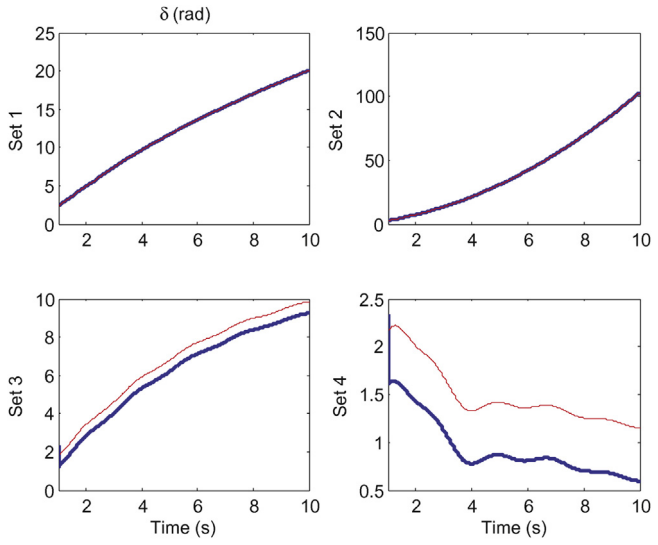

Fig. 6. The estimated rotor angle compared to the simulated rotor angel. Red line: Simulation results. Blue line: Estimated results. (For interpretation of the references to color in this figure legend, the reader is referred to the web version of the article.)

4.1. Two states and four parameters estimation

In this subsection, the formulated EKF algorithm in Section 3 will be tested. The initial gain matrix P is the co-variance matrix of the estimate error and P will be updated in EKF and converge to zero if EKF works. Hence the parameters in P are not important. However initial values of P matrix influence convergence rate. Therefore fine tuning is needed. Co-variance matrix Q represents noise co-variance. Noise includes processing noise and unmolded dynamics. Q is less deterministic. In often times superior filter performance can be obtained by "tuning" the filter parameters [38].

The co-variance matrix Q of the processing noise will be set differently for Sets 1 and 2 and Sets 3 and 4. Since Sets 1 and 2 are classical generator based simulation results and the internal voltage is fixed, there is no unmodeled dynamics in H, D and x'_d. Hence Q_{44}, Q_{55}, and Q_{66} are set to zero. On the other hand, Sets 3 and 4 are subtransient model based simulation data. Hence it is reasonable to model the unmodeled dynamics as noise in w_2, w_3, w_4, w_5, and w_6. The initial co-variance matrix is set to reflect the error in initial guess. Table 1 documents the parameters used in EKF estimation.

The rotor angle estimation matches very well with the simulated rotor angle in Sets 1 and 2 scenarios (Fig. 6). In Sets 3 and 4, there is a discrepancy between the estimation and the real value though the dynamic trends match each other well. The discrepancy can be explained by comparing the classical machine model versus a two-axis machine model (Fig. 7).

The two voltage sources are equivalent to each other [37]. Hence the classic model voltage source can be expressed by:

$$E = \sqrt{(E'^o_d + (x'_q - x'_d)I^o_q)^2 + (E'^o_q)^2} \tag{17}$$

Table 1
Covariance matrices for two-state four-parameter estimation.

P	Sets 1 and 2	Sets 3 and 4	Q	Sets 1 and 2	Sets 3 and 4
P_{11}	1	1	Q_{11}	$10^{-4}\Delta t$	$10^{-4}\Delta t$
P_{22}	30	30	Q_{22}	$10^{-3}\Delta t$	$10^{-3}\Delta t$
P_{33}	0.1	0.1	Q_{33}	0	0
P_{44}	5	5	Q_{44}	0	0
P_{55}	50	50	Q_{55}	0	0
P_{66}	1	1	Q_{66}	0	$0.01\Delta t$

where x'_q is the q axis transient reactance; E'^o_d, E'^o_q, and I'^o_q are the d and q axis components of the voltage source and the current during steady state.

$$\delta'^o = \tan^{-1}\left(\frac{E'^o_q}{E'^o_d + (x'_q - x'_d)I^o_q}\right) - \frac{\pi}{2} \tag{18}$$

We notice that there is always a difference between the angle of the classical generator and the rotor angle ($\delta - \gamma = \delta'^o$). Therefore, there is always a discrepancy (δ'^o) between the estimated rotor angle and the simulated rotor angle when the simulation model is subtransient model while the estimation model is a classical model.

The estimation of the rotor speed, the mechanical power, inertia constant, damping factor and transient reactance using Sets 1 and 2 data sets are found to be good matches of the simulation results. The results are shown in Figs. 8–12.

Sets 3 and 4 data are simulation data from subtransient generator model. Excitation control is not modeled for Set 3 data. For Set 3 data, the estimation of H is higher than the real value while for Set 4 data, the estimation of H is lower than the real value.

When the field voltage E_{fd} is constant, the effect of the synchronous machine field circuit dynamics such as the field flux variations causes a slight reduction in the synchronizing torque component and increase in the damping torque component [39] at the electromechanical oscillation modes. The linearized swing equation for a classical generator can be expressed as:

$$s^2(\Delta\delta) + \frac{D}{2H}s(\Delta\delta) + \frac{K_s}{2H}\omega_0(\Delta\delta) = \frac{\omega_0}{2H}\Delta P_m \tag{19}$$

where $K_s = \partial P_e/\partial\delta$, D is called the damping torque component while K_s is called the synchronizing torque component. Therefore, the characteristic equation is given by:

$$s^2 + \frac{D}{2H}s + \frac{K_s\omega_0}{2H} = 0 \tag{20}$$

The effect of field flux variations will change the synchronizing torque component and the damping torque component by decreasing K_s and increasing K_D. Detailed explanation can be referred in [37,39]. A brief explanation is offered in this paper. Considering the field flux variation, the linearized system model is shown in Fig. 13 [39], where K_1, K_2, K_3 and K_4 are constants related to operating conditions, T'_{d0} is the field winding time constant. From

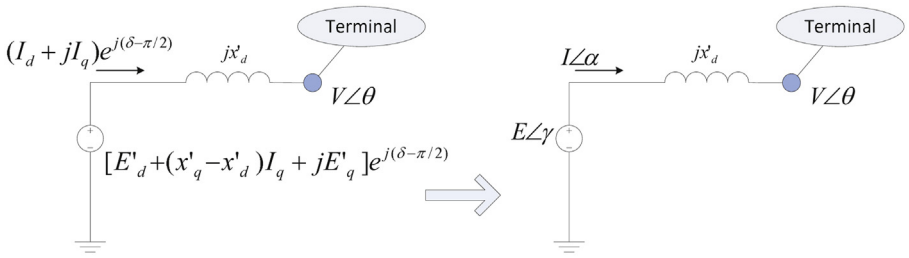

Fig. 7. Two-axis model versus a classic generator model.

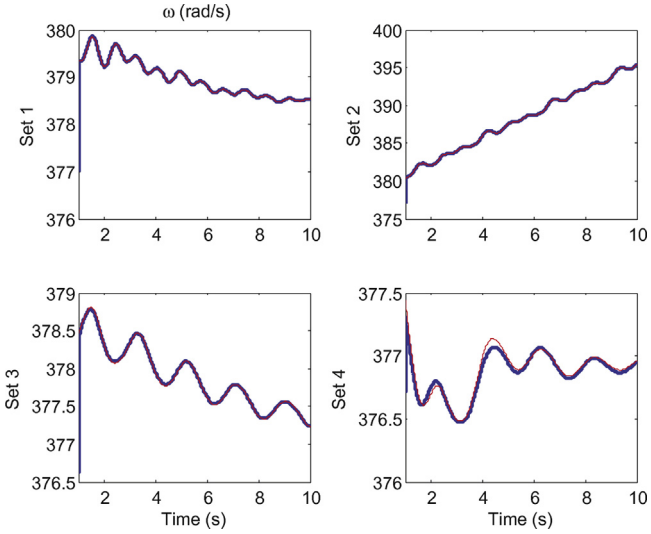

Fig. 8. The estimated rotor speed compared to the simulated rotor speed. Red line: Simulation results. Blue line: Estimated results. (For interpretation of the references to color in this figure legend, the reader is referred to the web version of the article.)

Fig. 13, we can find the contribution of K_s and K_D due to field flux variation or $\Delta E'_q$.

$$\frac{\Delta T_e}{\Delta\delta}|_{\text{due to}}\Delta E'_q = \frac{-K_2K_3K_4}{1+sK_3T'_{d0}} \tag{21}$$

Substituting s by $j\omega$ and we have:

$$\text{Re}\left[\frac{\Delta T_e}{\Delta\delta}\right] = \frac{-K_2K_3K_4}{1+\omega^2K_3^2T'^2_{d0}} \tag{22}$$

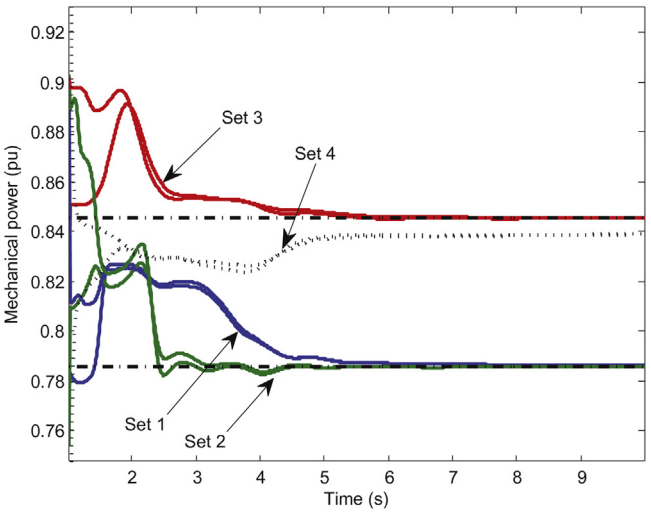

Fig. 9. The estimated mechanical power.

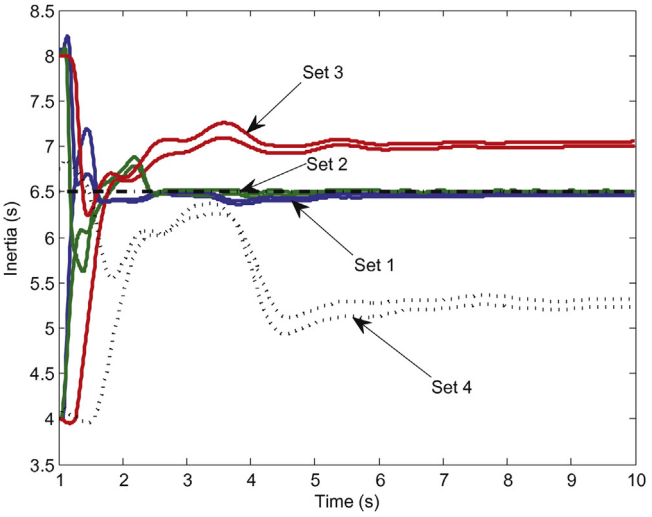

Fig. 10. The estimated damping factor.

$$\text{Im}\left[\frac{\Delta T_e}{\Delta\delta}\right] = \frac{K_2K_3^2K_4T'_{d0}}{1+\omega^2K_3^2T'^2_{d0}} \tag{23}$$

$$Im\left[\frac{\Delta T_e}{\Delta\delta}\right] \approx \frac{K_2K_4}{\omega T'_{d0}} \tag{24}$$

where K_2, K_3 and K_4 are positive numbers. Therefore, the impact of field flux variation can cause a decreased synchronizing torque component due to armature reaction while an increased damping torque component.

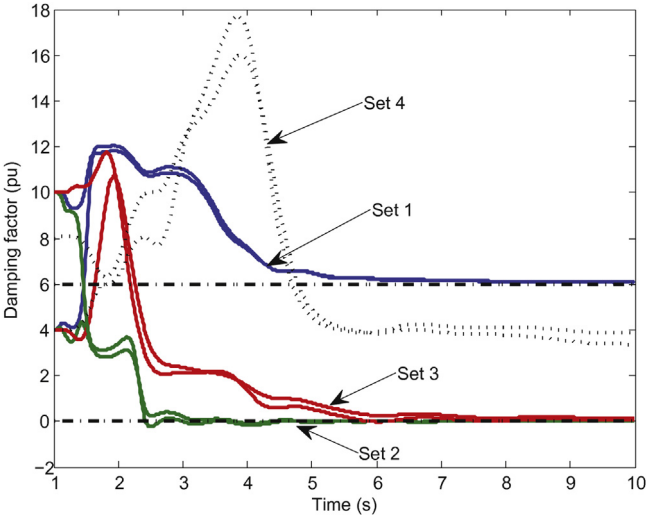

Fig. 11. The estimated inertia constant.

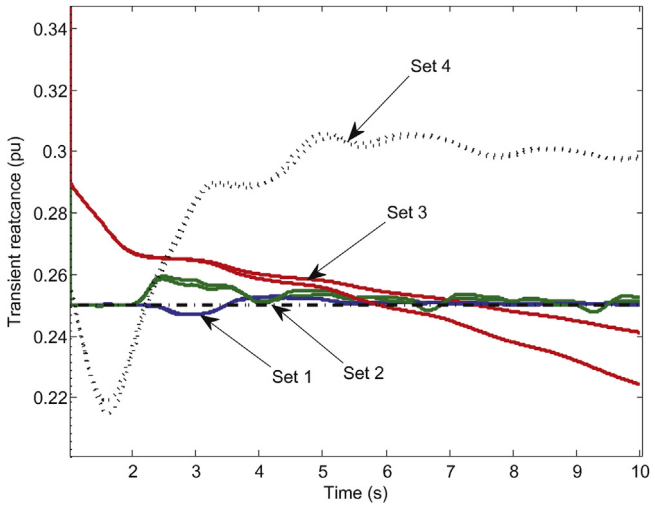

Fig. 12. The estimated transient reactance.

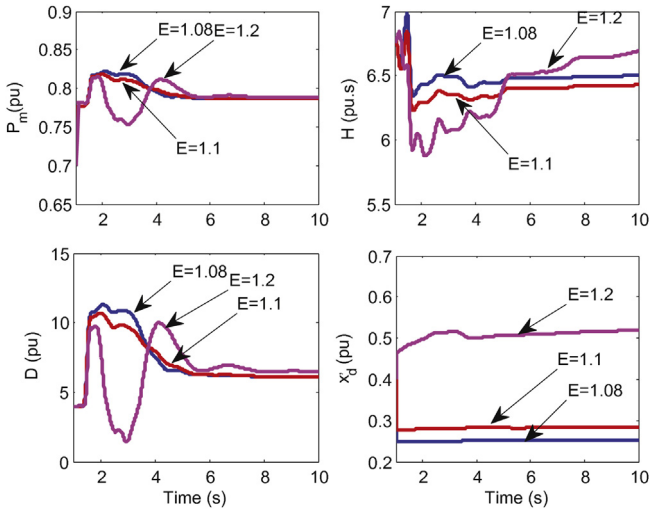

Fig. 14. Impact of E assumption on estimation.

For a classical generator model, it is assumed that $T'_{d0} \approx \infty$. When T'_{d0} is very large, there is no effect on the damping torque component.

The characteristic equation becomes:

$$s^2 + \frac{DK_{fD}}{2H}s + \frac{K_s K_{fs}\omega_0}{2H} = 0$$
$$\text{Or}: \quad s^2 + \frac{D'}{2H'}s + \frac{K_s\omega_0}{2H'} = 0 \tag{25}$$

where $K_{fD} > 1$ (increase in the damping torque component), $K_{fs} < 1$ (reduction in the synchronizing torque component), $H' = H/K_{fs} > H$, and $D' = DK_{fD}/K_{fs} > D$.

Therefore, it is reasonable for EKF-based estimation to find the estimated inertia and damping constant greater than the real values for Set 3 data.

The excitation control's effect on damping and synchronizing torque components at the oscillation frequency depends on the gain of the AVR and the system operating condition. In this case study, a high gain is chosen which introduces a positive synchronizing torque component and a negative damping torque component [39]. Compared to the effect of machine circuit dynamics, the effect of the AVR is much significant. Based on the same analysis carried out in (25), it can be found that $H' < H$ and $D' < D$. Therefore, for Set 4 data, it is reasonable that the estimated inertia constant and damping factor are less than the real values.

For this two-state four-parameter estimation problem, two initial guesses are used. Except for x'_d for Set 3, all parameter estimation converges to the same or close results within 10 s. Therefore, this EKF application is considered to be able to give converged and reasonable estimation.

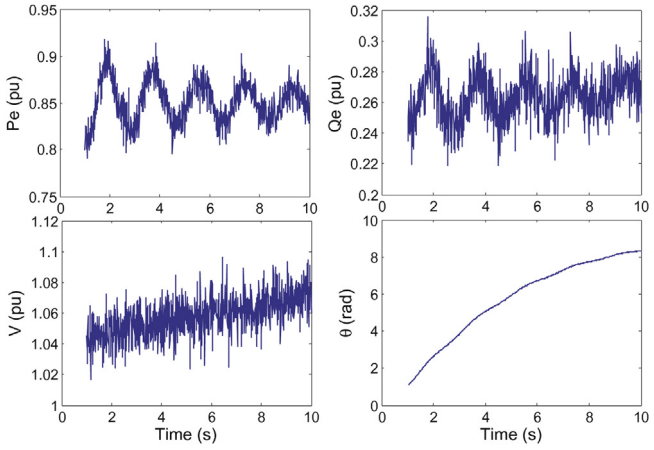

Fig. 15. The measurements.

4.2. Impact of the assumption of E

The impact of E assumption is shown in Fig. 14. Set 1 data is used for this test. Different E values are assumed: 1.08, 1.1 and 1.2. The true value of E is 1.08 pu. It can be observed that the value of E impacts the estimation of x'_d a good deal. Its impact on the other parameters such as P_m, H and D are much less significant.

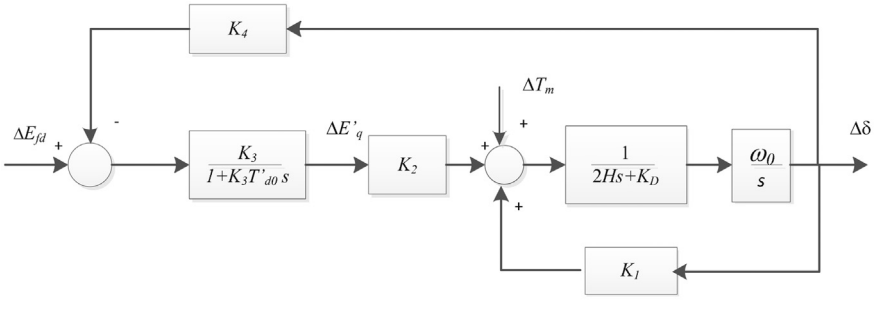

Fig. 13. Linearized synchronous generator model considering field flux variation.

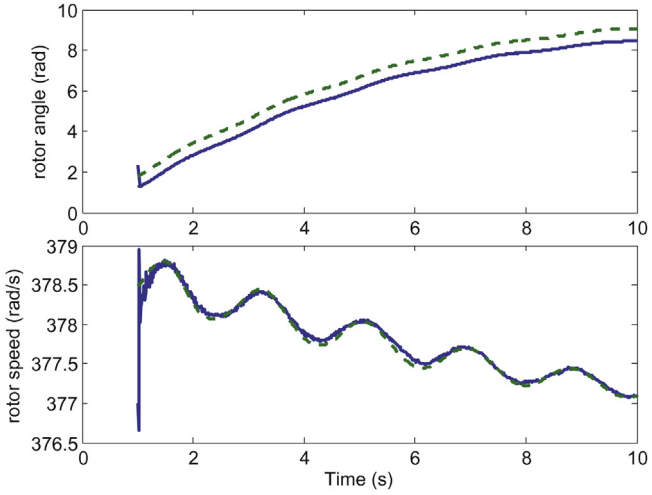

Fig. 16. The estimated states.

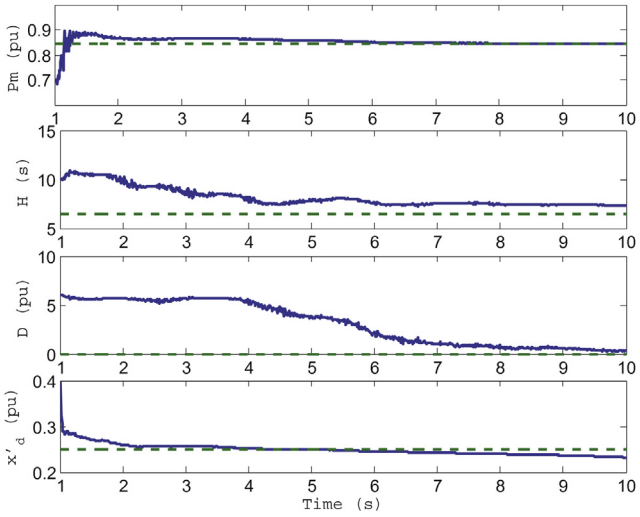

Fig. 17. The estimated parameters.

4.3. Two-state four-parameter estimation based on measurements with white noise

In this section, Set 3 data are assumed to be polluted by white noise. The measurements are presented in Fig. 15.

White noises are added on active power, reactive power and voltage. The estimated states and parameters are presented in Figs. 16 and 17.

It is found that the algorithm can estimate accurate states when there is noise. All parameters except H can be estimated accurately in 10 s. The estimation of H is greater than the true value due to modeling error which has been explained in the previous subsection.

5. Conclusion

In this paper, an EKF-based dynamic state and parameter estimation using model decoupling technique is investigated. The application can perform real-time dynamic estimation for subsystems using PMU data where the real and reactive powers are treated as the input to the estimation model while the voltage and phase angle are treated as the output from the estimation model. Based on a classic generator estimation model, the proposed EKF method can successfully estimate the states and parameters related to electromechanical dynamics. Simulation data generated from classical model, subtransient model and subtransient model equipped with AVR are used to test the estimation. It is demonstrated that the EKF-based estimation can give reasonable estimation for two-state four-parameter estimation.

References

[1] A. Phadke, J. Thorp, K. Karimi, State estimation with phasor measurements, IEEE Transactions on Power Systems 1 (1) (1986) 233–238.
[2] L. Vanfretti, J. Chow, D.E.S. Sarawgi, B. Fardanesh, A framework for estimation of power systems based on synchronized phasor measurement data, in: Proc. IEEE Power and Energy General Meeting, Calgary, CA, 2009.
[3] L. Zhao, A. Abur, Multiarea state estimation using state estimation with phasor measurements, IEEE Transactions on Power Systems 20 (2) (2005) 611–617.
[4] A. Agarwal, J. Ballance, B. Bhargava, J. Dyer, K. Martin, J. Mo, Real time dynamics monitoring system (RTDMS) for use with synchrophasor technology in power systems, in: Proc. IEEE Power & Energy General Meeting, 2011, pp. 1–6.
[5] Standard mod-013-1 – RRO Dynamics Data Requirements and Reporting Procedures, 2006 http://www.nerc.com/files/MOD0131.pdf
[6] M. Burth, G. Verghese, M. Velez-Reyes, Subset selection for improved parameter estimation in on-line identification of a synchronous generator, IEEE Transactions on Power Systems 14 (1) (1999) 218–225.
[7] J.J. Sanches-Gasca, C. Bridenbaugh, C. Bowler, J. Edmonds, Trajectory sensitivity based identification of synchronous generator and excitation system parameters, IEEE Transactions on Power Systems 3 (4) (1988) 1814–1821.
[8] M. Karrati, O. Malik, Identification of physical parameters of a synchronous generator from online measurements, IEEE Transactions on Energy Conversion 19 (2) (2004) 407–415.
[9] C.C. Lee, O. Tan, A weighted-least-squares parameter estimator for synchronous machines, IEEE Transactions on Power Systems 96 (1) (1977) 97–101.
[10] M. Namba, T. Nishiwaki, S. Yokokawa, K. Ohtsuka, Y. Ueki, Identification of parameters for power system stability analysis using Kalman filter, IEEE Transactions on Power Apparatus and Systems 100 (7) (1981) 3304–3310.
[11] J. Ma, B.W. Hogg, N. Zhiyuan, Y. Yihan, Online decoupled identification of transient and subtransient generator parameters, IEEE Transactions on Power Systems 9 (4) (1994) 1908–1914.
[12] Z. Zhao, F. Zheng, J. Gao, L. Xu, A dynamic online parameter identification and full-scale system experimental verification for large synchronous machines, IEEE Transactions on Energy Conversion 10 (3) (1995) 392–398.
[13] R. Wamkeue, C. Jolette, A. Mabwe, I. Kamwa, Cross-identification of synchronous generator parameters from RTDR test time-domain analytical responses, IEEE Transactions on Energy Conversion 26 (3) (2011) 776–786.
[14] S.M. Benchluch, J. Chow, A trajectory sensitivity method for the identification of nonlinear excitation system models, IEEE Transactions on Energy Conversion 8 (2) (1993) 159–164.
[15] J. Melgoza, G. Heydt, A. Keyhani, B. Agrawal, D. Selin, Synchronous machine parameter estimation using the Hartley series, IEEE Transactions on Energy Conversion 16 (1) (2001) 49–54.
[16] E. Kyriakides, G. Heydt, V. Vittal, Online parameter estimation of round rotor synchronous generators including magnetic saturation, IEEE Transactions on Energy Conversion 20 (3) (2005) 529–537.
[17] J. Melgoza, G. Heydt, A. Keyhani, B. Agrawal, D. Selin, An algebraic approach for identifying operating point dependent parameters of synchronous machines using orthogonal series expansions, IEEE Transactions on Energy Conversion 16 (1) (2001) 92–98.
[18] E. Kyriakides, G. Heydt, V. Vittal, On-line estimation of synchronous generator parameters using a damper current observer and a graphic user interface, IEEE Transactions on Energy Conversion 19 (3) (2004) 499–507.
[19] E. Eitelberg, R.G. Harley, Estimating synchronous machine electrical parameters from frequency response tests, IEEE Transactions on Energy Conversion 2 (1) (1987) 132–136.
[20] R. Escarela-Perez, T. Niewierowicz, E. Campero-Littlewood, Synchronous machine parameters from frequency–response finite-element simulations and genetic algorithms, IEEE Transactions on Energy Conversion 16 (2) (2001) 198–203.
[21] A. Keyhani, S. Hao, R.P. Schulz, Maximum likelihood estimation of generator stability constants using SSFR test data, IEEE Transactions on Energy Conversion 16 (1) (1991) 140–154.
[22] I. Kamwa, P. Viarouge, H. Le-Huy, J. Dickinson, A frequency domain maximum likelihood estimation of synchronous machine high order models using SSFR test data, IEEE Transactions on Energy Conversion 7 (3) (1992) 525–536.
[23] E. Ghahremani, I. Kamwa, Dynamic state estimation in power system by applying the extended Kalman filter with unknown inputs to phasor measurements, IEEE Transactions on Power Systems 26 (4) (2011) 2556–2566.
[24] E. Ghahremani, I. Kamwa, Online state estimation of a synchronous generator using unscented Kalman filter from phasor measurements units, IEEE Transactions on Energy Conversion 26 (4) (2011) 1099–1108.
[25] Z. Huang, K. Schneider, J. Nieplocha, Feasibility studies of applying Kalman filter techniques to power system dynamic state estimation, in: Proc. International Power Engineering Conference (IPEC), 2007, pp. 376–382.

[26] Z. Huang, P. Du, D. Losterev, B. Yang, Application of extended Kalman filter techniques for dynamic model parameter calibration, in: Proc. IEEE Power & Energy General Meeting, 2009, pp. 1–6.
[27] K. Kalsi, Y. Sun, Z. Huang, P. Du, R. Diao, K. Anderson, Y. Li, B. Lee, Calibrating multi-machine power system parameters with the extended Kalman filter, in: Proc. IEEE Power & Energy General Meeting, 2011, pp. 1–6.
[28] Z. Huang, D. Kosterev, R. Guttronmson, T. Nguyen, Model validation with hybrid dynamic simulation, in: Proc. IEEE Power Engineering Society General Meeting, 2006, pp. 1–6.
[29] P. Du, Z. Huang, R. Diao, B. Lee, K. Anderson, Application of Kalman filter to improve model integrity for securing electricity delivery, in: IEEE/PES Power Systems Conference and Exposition (PSCE), 2011, pp. 1–6.
[30] J.H. Chow, A.C. Chakrabortty, L. Vanfretti, M. Arcak, Estimation of radial power system transfer path dynamic parameters using synchronized phasor data, IEEE Transactions on Power Systems 23 (2) (2008) 564–571.
[31] F. Okou, L.-A. Dessaint, O. Akhrif, Power systems stability enhancement using a wide-area signals based hierarchical controller, IEEE Transactions on Power Systems 20 (3) (2005) 1465–1477.
[32] J. Chapman, M. Ilic, C.K. nd, L. Eng, H. Kaufman, Stabilizing a multimachine power system via decentralized feedback linearizing excitation control, IEEE Transactions on Power Systems 8 (3) (1993) 830–839.
[33] M.S. Grewal, A.P. Andrews, Kalman Filtering: Theory and Practice Using Matlab, John Wiley & Sons, Inc., Hoboken, New Jersey, 2008.
[34] D. Simon, Optimal State Estimation, Wiley-Interscience, John Wiley & Sons, Inc., Hoboken, New Jersey, 2006.
[35] M. Klein, G. Rogers, P. Kundur, A fundamental study of inter-area oscillations in power systems, IEEE Transactions on Power Systems 6 (1991) 914–921.
[36] J.H. Chow, K.W. Cheung, A toolbox for power system dynamics and control engineering education and research, IEEE Transactions on Power Systems 7 (4) (1992) 1559–1564.
[37] P. Sauer, M. Pai, Power System Dynamics and Stability, Prentice Hall, Upper Saddle River, NJ, 1998.
[38] G. Welch, G. Bishop, An Introduction to the Kalman Filter, 2006 http://www.cs.unc.edu/welch/media/pdf/kalman_intro.pdf
[39] P. Kundur, Power System Stability and Control, McGraw-Hill, New York, USA, 1994.